

Margaret A. Livingstone · Victoria M. Kaspi · Fotis P. Gavriil · Richard
N. Manchester · E.V. Gotthelf · Lucien Kuiper

New Phase-coherent Measurements of Pulsar Braking Indices

Received: date / Accepted: date

Abstract Pulsar braking indices offer insight into the physics that underlies pulsar spin-down. Only five braking indices have been measured via phase-coherent timing; all measured values are less than 3, the value expected from magnetic dipole radiation. Here we present new measurements for three of the five pulsar braking indices, obtained with phase-coherent timing for PSRs J1846–0258 ($n = 2.65 \pm 0.01$), B1509–58 ($n = 2.839 \pm 0.001$) and B0540–69 ($n = 2.140 \pm 0.009$). We dis-

cuss the implications of these results and possible physical explanations for them.

Keywords Pulsars · Timing

PACS 95.85.Nv · 97.60.Gb

M. Livingstone
Physics Department, McGill University
Rutherford Physics Building
3600 University Street
Montreal, Qc H3A 2T8
Canada
E-mail: maggie@physics.mcgill.ca

V.M. Kaspi
Physics Department, McGill University
Rutherford Physics Building
3600 University Street
Montreal, Qc H3A 2T8
Canada

F.P. Gavriil
NASA Goddard Space Flight Center
Code 662, X-ray Astrophysics Laboratory
Greenbelt, MD 20771

R.N. Manchester
Australia National Telescope Facility
CSIRO
P.O. Box 76
Epping NSW 1710
Australia

E.V. Gotthelf
Columbia Astrophysics Laboratory
Columbia University
550 West 120th Street
New York, NY
10027-6601

L. Kuiper
Netherlands Institute for Space Research
Sorbonnelaan 2
3584 CA
Utrecht, Netherlands

1 Introduction

A very commonly assumed model for pulsar spin-down posits that

$$\dot{\nu} = -K\nu^n, \quad (1)$$

where ν is the pulse frequency, $\dot{\nu}$ is the frequency derivative, K is a constant and n is the braking index. The braking index is then given by

$$n = \frac{\nu\ddot{\nu}}{\dot{\nu}^2}. \quad (2)$$

The braking index provides insight into the physics that drives pulsar spin-down. Typically, it is assumed that magnetic dipole radiation underlies pulsar evolution, resulting in $n = 3$ (e.g. Manchester & Taylor 1977). However, other processes could, in principle, cause the pulsar to radiate and would result in different values for n and K . For example, a pulsar spun down entirely by the loss of relativistic particles would have $n = 1$ (Michel & Tucker 1969). A pulsar losing energy via gravitational radiation or quadrupole magnetic radiation would spin down with $n = 5$ (Blandford & Romani 1988).

Braking indices have proven difficult to measure. To date, only six have been reported even though more than 1600 pulsars are known. Evidently, the pulsar properties necessary for a measurement of n are rare; the pulsar must: spin down quickly; experience few, small, and relatively infrequent glitches; and be relatively uncontaminated by timing noise, a low-frequency stochastic process superposed on the deterministic spin-down of the pulsar. The youngest pulsars, of which the Crab pulsar is the most famous example, uniquely possess these three qualities. The reason then for the paucity of measured

values of n is a direct consequence of the relative rarity of very young pulsars, i.e. those with characteristic ages on the order of 1 kyr, where characteristic age is defined as

$$\tau_c \equiv \frac{P}{2\dot{P}} = \frac{\nu}{2\dot{\nu}}. \quad (3)$$

Of the six pulsars with measured n , five were obtained via phase-coherent timing. All five of these pulsars: PSRs J1846–0258, B0531+21 (the Crab pulsar, $n = 2.51 \pm 0.01$), B1509–58, J1119–6127 ($n = 2.91 \pm 0.05$), and B0540–69, have characteristic ages less than 2 kyr (Livingstone et al. 2006; Lyne et al. 1993; Livingstone et al. 2005b; Camilo et al. 2000; Livingstone et al. 2005a). The sixth measurement, that of the Vela pulsar ($n = 1.4 \pm 0.2$), could not be obtained with phase-coherent timing due to large glitches (Lyne et al. 1996). Timing noise and large glitches begin to seriously contaminate measurements of n when pulsars have characteristic ages ~ 5 kyr (McKenna & Lyne 1990; Marshall et al. 2004).

In this paper we report on long-term *Rossi X-ray Timing Explorer* observations of three young pulsars, PSRs J1846–0258, B1509–58 and B0540–69. We present braking index measurements for each of these pulsars obtained via phase-coherent timing.

2 Phase-coherent pulsar timing

The most accurate method of extracting pulsar timing parameters is phase-coherent timing, that is, accounting for every turn of the pulsar. Pulse times of arrival (TOAs) are measured and fitted to a Taylor expansion of pulse phase, ϕ at time t given by

$$\phi(t) = \phi(t_0) + \nu_0(t-t_0) + \frac{1}{2}\dot{\nu}_0(t-t_0)^2 + \frac{1}{6}\ddot{\nu}_0(t-t_0)^3 + \dots, \quad (4)$$

where subscript 0 denotes a parameter at the reference epoch, t_0 . TOAs and initial spin parameters are input to pulse timing software (e.g. TEMPO¹) and refined spin parameters and timing residuals are output.

The existence of timing noise and glitches in young pulsars is well known to contaminate the measurement of deterministic spin parameters. Though powerful, a fully phase-coherent timing solution can be sensitive to these contaminants. In such cases, a partially coherent method may be employed. In this case, local phase-coherent measurements of ν , $\dot{\nu}$ and possibly $\ddot{\nu}$ are made. Though the effects of timing noise cannot be eliminated, the noise component is more readily identified and separated from the deterministic component of the spin-down, as shown in Section 5. In addition, glitches can be easier to identify with this method, as will be shown in Section 6 of this paper.

3 Observations

In this paper we describe observations of three young pulsars PSRs J1846–0258, B1509–58, and B0540–69 taken with the Proportional Counter Array (PCA) on board the *Rossi X-ray Timing Explorer* (RXTE). The PCA consists of five collimated xenon/methane multianode proportional counter units (PCUs). The PCA operates in the 2–60 keV energy range, has an effective area of ~ 6500 cm² and has a 1 degree field of view. While RXTE has no imaging capability, it has excellent time resolution of $\sim 1 \mu\text{s}$ (Jahoda et al. 1996). This makes RXTE ideal for observing young, rapidly rotating pulsars.

Observations of PSR B1509–58 were taken in “GoodXenonWithPropane” mode, while observations of the other two sources were taken in “GoodXenon” mode. Both modes record the photon arrival time with $1\mu\text{s}$ -resolution and photon energy with 256-channel resolution. The number of PCUs active during an observation varies, but is typically three. For PSRs B1509–58 and J1846–0258, which have relatively hard spectra, all three Xenon layers and photons with energies ranging from 2–60 keV were used, while for the softer spectrum source, PSR B0540–69, only the top Xenon layer and photons with energies ranging from 2–18 keV were used. Further details of X-ray and radio observations of PSR B1509–58 are given in Livingstone et al. (2005b) and references therein. Details of RXTE observations of PSR B0540–69 can be found in Livingstone et al. (2005a) while details of PSR J1846–0258 observations can be found in Livingstone et al. (2006) and references therein.

Data were reduced using standard FITS tools as well as in-house software developed for analyzing RXTE data for pulsar timing. Data from different PCUs were merged and binned at (1/1024) s resolution. Photon arrival times were corrected to barycentric dynamical time (TDB) at the solar system barycenter using the J2000 source positions and the JPL DE200 solar system ephemeris.

For PSRs B0540–69 and J1846–0258, initial ephemerides were found by performing periodograms on observations to determine values of ν . Several values of ν were fitted with a linear least squares fit to determine an initial value of $\dot{\nu}$. These initial values were then used as input to a Taylor expansion of TOAs to determine more accurate parameters (Eq. 4). PSR B1509–58 has a previously determined ephemeris from radio timing data obtained with the Molonglo Observatory Synthesis Telescope and the Parkes Radio Telescope (Kaspi et al. 1994). We were able to extend that fit with 7.6 yr of RXTE data, removing a constant, but not well determined, offset between radio and X-ray TOAs.

4 PSR J1846–0258

PSR J1846–0258 is a very young pulsar ($\tau_c = 723$ yr) located at the center of the supernova remnant Kesteven

¹ <http://www.atnf.csiro.au/research/pulsar/tempo>

Table 1 Spin parameters for PSR J1846–0258

Parameter	First solution	Second solution
Dates (MJD)	51574.2 - 52837.4	52915.8 - 53578.6
Epoch (MJD)	52064.0	53404.0
ν (s^{-1})	3.0782148166(9)	3.070458592(1)
$\dot{\nu}$ (10^{-11}s^{-2})	-6.71563(1)	-6.67793(5)
$\ddot{\nu}$ (10^{-21}s^{-3})	3.87(2)	3.89(4)
Braking Index (n)	2.64(1)	2.68(3)
Glitch epoch (MJD)	52210(10)	
$\Delta\nu/\nu$	$2.5(2) \times 10^{-9}$	
$\Delta\dot{\nu}/\dot{\nu}$	$9.3(1) \times 10^{-4}$	

75. It has a relatively long spin period of 324 ms and a large magnetic field² of $B \sim 5 \times 10^{13}$ G. PSR J1846–0258 has been observed with RXTE for 6.3 yr since its discovery in 1999 (Gotthelf et al. 2000).

Using our initial ephemeris we obtained a phase-coherent timing solution valid over a 3.5-yr interval in the range MJD 51574–52837. Three spin parameters (ν , $\dot{\nu}$ and $\ddot{\nu}$) were required by the fit. In addition, we discovered a small glitch near MJD 52210 \pm 10. The fitted glitch parameters are $\Delta\nu/\nu = 2.5(2) \times 10^{-9}$ and $\Delta\dot{\nu}/\dot{\nu} = 9.3(1) \times 10^{-4}$. Note that these and all other quoted uncertainties are 68% confidence intervals, unless otherwise indicated. The wide spacing of data near the glitch prevent the detection of any short-timescale glitch recovery. Timing residuals are shown in Figure 1. The top panel of Figure 1 shows residuals with ν , $\dot{\nu}$, $\ddot{\nu}$ and glitch parameters fitted. The residuals clearly show systematics due to timing noise and possibly unmodeled glitch recovery. In order to minimize contamination of long-term timing parameters, we fitted additional frequency derivatives to render the residuals consistent with Gaussian distributed residuals (a process known as ‘whitening’ residuals. See, for example, Kaspi et al. 1994). For this timing solution, a total of eight frequency derivatives were fitted, shown in the bottom panel of Figure 1. The braking index resulting from this ‘whitened’ timing solution is $n = 2.64 \pm 0.01$. Complete spin-down parameters are given in Table 1.

Phase was lost over a 78-day gap in the data near MJD 52837, indicated by the fact that a timing solution attempting to connect over this gap fails to predict the pulse frequency at previous epochs. The loss of phase is likely due to timing noise or a second glitch. However, these two possibilities cannot be distinguished due to the relatively long gap in the data set.

A second phase-coherent timing solution was obtained for 1.8 yr from MJD 52915–53579 with ν , $\dot{\nu}$ and $\ddot{\nu}$. Timing residuals with these three parameters fit are shown in the top panel of Figure 2. Again, systematics due to timing noise and/or glitch recovery remain in these residuals. To ‘whiten’ timing residuals, five total frequency derivatives were fitted from the data, shown in the bottom panel

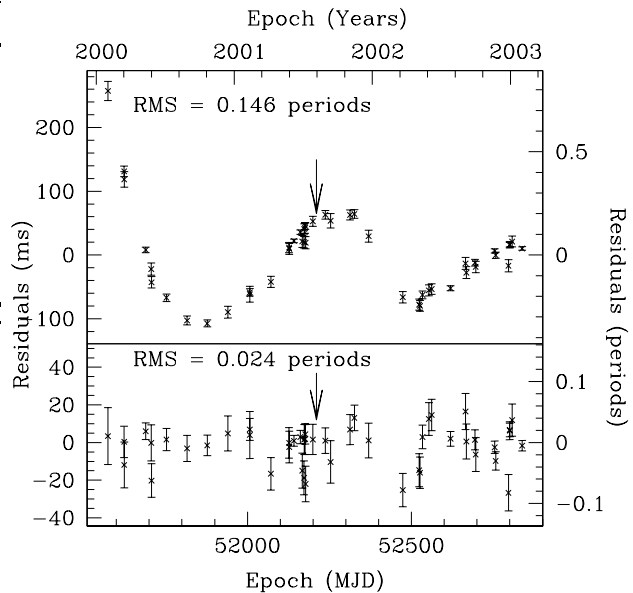


Fig. 1 Phase-coherent X-ray timing analysis of the young pulsar PSR J1846–0258 spanning a 3.5-yr interval in the range MJD 51574–52837 (after Livingstone et al. (2006)). Top panel: Residuals with ν , $\dot{\nu}$, $\ddot{\nu}$ as well as glitch parameters $\Delta\nu$ and $\Delta\dot{\nu}$ fitted. The glitch epoch, MJD 52210 is indicated by the arrow. Bottom panel: Residuals with glitch parameters and eight frequency derivatives in total fitted to render the residuals consistent with Gaussian noise.

of Figure 2. Complete spin parameters for this timing solution are given in Table 1.

Quoting the average value of n from the two independent timing solutions, which are in agreement, gives $n = 2.65 \pm 0.01$. As is the case for all measured values of n , this value is significantly less than 3, the value consistent with spin-down via magnetic dipole radiation. This implies that some other physical process must contribute to the spin-down of all of these pulsars.

This measurement of n for PSR J1846–0258 increases its age estimate (Livingstone et al. 2006). The commonly known characteristic age (Eq. 3) implicitly assumes that $n = 3$. A more physical estimate can be made once n is known. The age then can be estimated as

$$\tau = \frac{1}{n-1} \tau_c \leq 884 \text{ yr.} \quad (5)$$

The estimate is an upper limit since the initial spin frequency of the pulsar is not known. The upper limit approaches an equality when the pulsar is born spinning much faster than its present spin frequency. Given the long period of the pulsar and the estimated initial spin period distribution (e.g. Faucher-Giguère & Kaspi 2006), the latter is likely to have occurred. This age estimate for PSR J1846–0258 is less than the known age of the Crab pulsar of 952 yr.

² $B \equiv 3.2 \times 10^{19} (P\dot{P})^{1/2} \text{ G}$

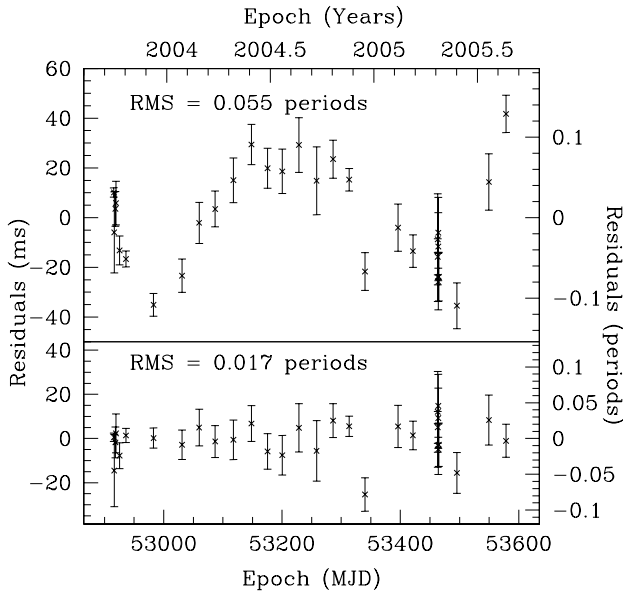


Fig. 2 Phase-coherent X-ray timing analysis of PSR J1846–0258 spanning an 1.8-yr interval from MJD 52915–53579 (after Livingstone et al. (2006)). Top panel: Residuals with ν , $\dot{\nu}$, $\ddot{\nu}$ fitted. Bottom panel: Residuals with five frequency derivatives total fitted to render the residuals consistent with Gaussian noise.

5 PSR B1509–58

The young pulsar PSR B1509–58 was discovered in 1982 and has been observed regularly ever since, first with radio telescopes such as the Molonglo Observatory Synthesis Telescope (Manchester et al. 1985) and the Parkes Radio Observatory (Kaspi et al. 1994), and more recently with RXTE (Rots 2004; Livingstone et al. 2005b). We phase-connected all 21.3 yr of available radio and X-ray timing data to determine the braking index. Timing residuals are shown in Figure 3. The top panel shows the timing residuals with ν and three frequency derivatives fitted; the middle panel shows residuals with the fourth frequency derivative also fitted; the bottom panel shows timing residuals with five frequency derivatives fitted. Remarkably for such a young pulsar, *no* glitches were detected in this time period. Spin parameters from this phase-coherent analysis are $\nu = 6.633598804(3) \text{ s}^{-1}$, $\dot{\nu} = -6.75801754(4) \times 10^{-11} \text{ s}^{-2}$, $\ddot{\nu} = 1.95671(2) \times 10^{-21} \text{ s}^{-3}$ at epoch MJD 49034.5. These parameters imply a braking index of $n = 2.84209(3)$, though timing noise that could not be completely removed by fitting additional frequency derivatives contributes to a systematic uncertainty that is not included in the formal uncertainty quoted here. To solve this problem, we performed a partially phase-coherent analysis by making independent measurements of n .

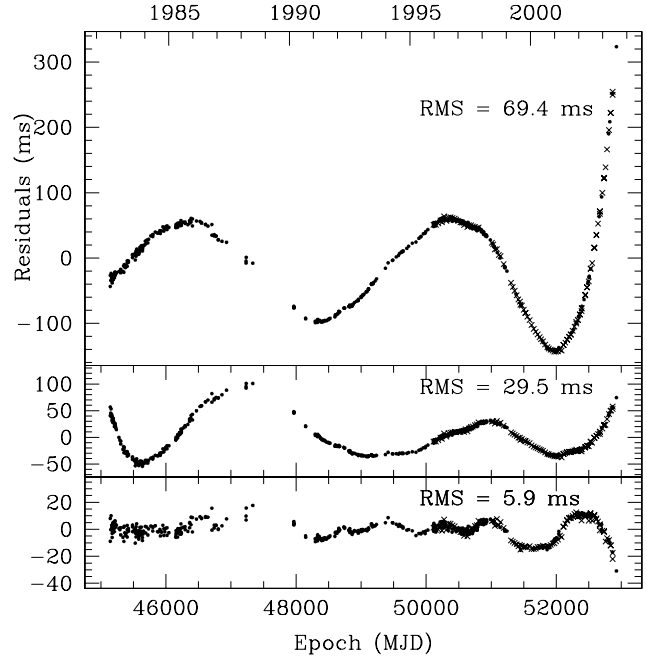


Fig. 3 Timing residuals for PSR B1509–58. Radio TOAs are shown as dots and the X-ray TOAs are shown as crosses (after Livingstone et al. (2005b)). The top panel has pulse frequency and three frequency derivatives removed, the middle panel also has the fourth frequency derivative removed, and the bottom panel shows residuals after the removal of five frequency derivatives.

Due to the large value of $\dot{\nu}$ for this pulsar, a significant measurement of n can be made in approximately 2 yr, without noticeable contamination of the measured spin parameters from timing noise. Thus, having over 20 years of data allows 10 independent measurements of n , which are shown in Figure 4. No secular variation of n over 21.3 yr is seen, however, there is significant deviation from the average value of $n = 2.839 \pm 0.003$. This uncertainty was determined by a ‘bootstrap’ analysis which is a robust method of determining uncertainties when the formal uncertainties are thought to underestimate the true values, i.e. due to the presence of timing noise (Efron 1979). Note that this value is in agreement with that obtained with the fully phase-coherent timing solution, as well as the previously reported value of $n = 2.837 \pm 0.001$ (Kaspi et al. 1994). The reduced χ^2 is 15 for 9 degrees of freedom. This variation is likely due to the same timing noise process that can be observed in timing residuals. Here, the variation is at the $\sim 1.5\%$ level. A similar analysis has been performed for PSR J1846–0258 where variations are seen to be on the order of $\sim 5\%$, though only at the 2σ level (Livingstone et al. 2006) and for the Crab pulsar where variations are on the order of 0.5% (Lyne et al. 1993).

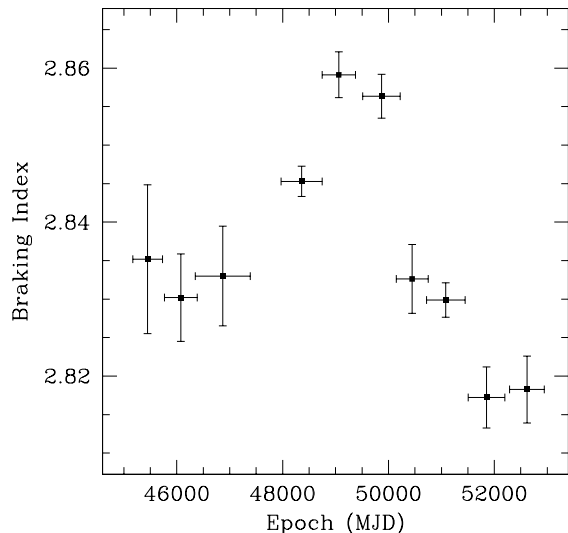


Fig. 4 Braking index calculated at 10 epochs of ~ 2 yr in length (after Livingstone et al. (2005b)). There is no statistically significant secular change of 21.3 yr of data. The average value is 2.839 ± 0.003 , in agreement with the previously reported value (Kaspi et al. 1994) and the value obtained from a phase-coherent analysis. The reduced χ^2 value is 15 for 9 degrees of freedom, suggesting contamination by timing noise.

6 PSR B0540–69

Located in the Large Magellanic Cloud, PSR B0540–69 is commonly known as the ‘Crab Twin’, due to its similar spin and nebular properties. For instance, its period of 50 ms and magnetic field $B \sim 5 \times 10^{12}$ G are nearer to those of the Crab pulsar ($P = 33$ ms, $B \sim 4 \times 10^{12}$ G) than for any other pulsar. Due to its large distance, PSR B0540–69 is very difficult to detect in the radio waveband (Manchester et al. 1993), hence regular radio timing of this source is not practical.

The lack of regular, long-term timing observations for this pulsar has led to conflicting values of n in the literature; reported values range from $n = 1.81 \pm 0.07$ to $n = 2.74 \pm 0.01$ (Zhang et al. 2001; Ögelman & Hasinger 1990). Widely spaced timing observations greatly increases the risk of losing phase if a phase-coherent solution is attempted. If instead of a phase-coherent timing solution, measurements of frequency are obtained over widely spaced intervals, small glitches can easily be missed and the effects of timing noise are difficult to discern. Two conflicting values of n are of particular interest since they are based on overlapping data from RXTE.

Zhang et al. (2001) reported on 1.2 years of regular timing observations and found a small magnitude glitch at MJD 51325 ± 45 with parameters $\Delta\nu/\nu = (1.90 \pm 0.04) \times 10^{-9}$ and $\Delta\dot{\nu}/\dot{\nu} = (8.5 \pm 0.5) \times 10^{-5}$. They used

the 300 days of data available after the glitch to measure a braking index of $n = 1.81 \pm 0.07$. Cusumano et al. (2003) extended the data set to 4.6 yr and reported that no glitch occurred. In contrast to the previous value, they measured $n = 2.125 \pm 0.001$.

We re-examined all previously reported RXTE data and extended the data set by 3 yr in order to resolve the discrepant timing solutions and measure the true braking index for this source. We phase connected a total of 7.6 yr of data and found a small glitch near MJD 51335 with parameters $\Delta\nu/\nu \sim 1.4 \times 10^{-9}$ and $\Delta\dot{\nu}/\dot{\nu} \sim 1.33 \times 10^{-4}$, in agreement with those reported by Zhang et al. (2001). This glitch is very small, and is most easily seen by the change in $\dot{\nu}$ at the glitch epoch. Figure 5 shows 22 measurements of $\dot{\nu}$ obtained from individual phase-coherent analyses, with the fitted glitch epoch indicated by an arrow. The slope of the line, that is, the second frequency derivative $\ddot{\nu}$, does not change significantly after the glitch (before $\ddot{\nu} = 3.81(3) \times 10^{-21} \text{s}^{-3}$, after $\ddot{\nu} = 3.81(1) \times 10^{-21} \text{s}^{-3}$). Uncertainties on $\ddot{\nu}$ were determined by a bootstrap analysis (Efron 1979). We use the average to determine the braking index, found to be $n = 2.140 \pm 0.009$.

In agreement with Zhang et al. (2001), we report a small glitch near MJD 51335, though our value of n is significantly larger. By phase-connecting only the same 300 day subset of data that they used to measure n , we find $n = 1.82 \pm 0.01$, in agreement with their result. The low value of n in this case appears to be the result of timing noise and/or glitch recovery contaminating the relatively short time baseline used to measure n .

Our measured value of n is 1.7σ from that reported by Cusumano et al. (2003, $n = 2.125 \pm 0.001$) though they do not report a glitch and their uncertainty does not account for the effects of timing noise. The reason for the agreements between our measured values is that their value of n was determined by two phase-coherent fits to the data, before and after the glitch epoch reported by Zhang et al. (2001), despite the fact that Cusumano et al. (2003) report no glitch.

7 Implications and Physical Explanations for $n < 3$

All measured values of n are less than 3, the value consistent with spin-down due solely to magnetic dipole radiation. This implies that an additional torque is contributing to the spin-down of young pulsars. Also intriguing is the relatively wide range of measured values of n , shown in Table 2. A measurement of n immediately provides a correction to the age estimate of the pulsar given by the characteristic age, as shown with Equation 5. Comparisons of the characteristic age and age estimated with n are also given in Table 2. Although the age estimate is always increased with a measurement of $n < 3$, it should be noted that the age estimates given are upper

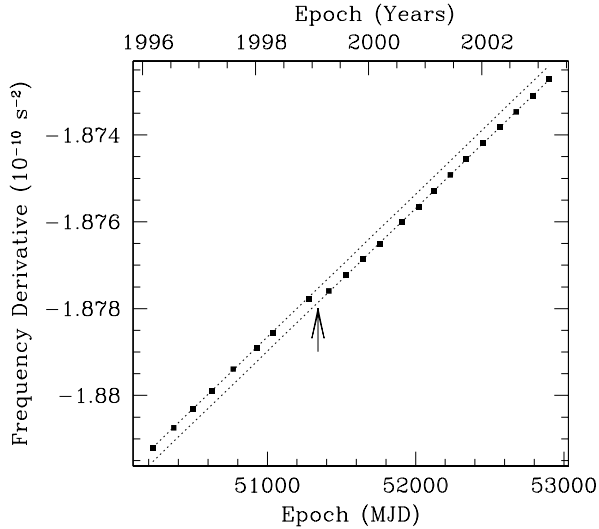


Fig. 5 Measurements of $\dot{\nu}$; the slope is $\ddot{\nu}$ (after Livingstone et al. (2005a)). The glitch occurring near MJD 51342 is shown with an arrow. The pre-glitch slope is $\ddot{\nu} = 3.81(3) \times 10^{-21} \text{s}^{-3}$, while the post-glitch slope is $\ddot{\nu} = 3.81(1) \times 10^{-21} \text{s}^{-3}$. The average of pre- and post-glitch n is 2.140 ± 0.009 . Measurement uncertainties are smaller than the points.

Table 2 Braking index measurements via phase-coherent timing. Also given are the characteristic age, τ_c and age estimate using n , τ .

Pulsar	n	τ_c	τ
J1846–0258	2.65(1)	723	884
B0531+21	2.51(1)	1240	1640
B1509–58	2.839(3)	1550	1690
J1119–6127	2.91(5)	1610	1680
B0540–69	2.140(9)	1670	2940

limits since the initial spin frequencies are not known. The calculation of magnetic fields are also affected by a measurement of $n < 3$, since these are obtained assuming pure magnetic dipole radiation. Unfortunately, there is no simple formula to estimate the correction to the dipole magnetic field as there is for the age. Specific details of the spin-down torque are required to uncover the true magnetic field of pulsars.

There are several theories that attempt to explain the measurements of $n < 3$. One explanation is that the pulsar’s magnetic field grows or counter-aligns with the spin axis. This is equivalent to allowing the ‘constant’, K , in the simple model of pulsar spin down (Eq. 1) to vary with time (Blandford & Romani 1988). An advantage of this model is that it can be tested if precision measurements of the third frequency derivative can be made (Blandford

1994). To date, the third frequency derivative has been measured only for the Crab pulsar (Lyne et al. 1993) and PSR B1509–58 (Livingstone et al. 2005b), though neither is known with sufficient precision to rule out the null hypothesis of a constant value of K . Timing noise and in the case of the Crab pulsar, glitches, may prevent a sufficiently precise measurement from ever being made.

Another suggestion is that a fall-back disk formed from supernova material modulates the spin-down of young pulsars, providing a propeller torque in addition to the torque from magnetic dipole radiation. This would cause the pulsar to lose energy more quickly leading to a measured value $2 < n < 3$ (Alpar et al. 2001). A difficulty in this model is that the disk must not suppress the pulsed radio emission during the propeller phase (Menou et al. 2001).

In recent years, much work has been done on modelling the pulsar magnetosphere. Fully physical, three dimensional, time-dependent models of the pulsar magnetosphere are still some time away, however, significant progress has been made and there is some suggestion that $n < 3$ may be a natural result of a plasma filled magnetosphere (see, for example Spitkovsky 2005; Timokhin 2006; Contopoulos & Spitkovsky 2006).

The idea that plasma in the magnetosphere affects the torque acting on a pulsar is gaining acceptance with the first observational evidence for this having recently being presented. Kramer et al. (2006) show that PSR B1931+24, which has curious quasi-periodic nulling behaviour, spins down at different rates when it is ‘on’ or ‘off’. Specifically, the pulsar has a faster rate of spin down when it is observed in the radio waveband than when it goes undetected. This implies a connection between the radio emission mechanism and the spin-down torque. The interpretation presented by the authors is that the radio emission mechanism is only active when sufficient plasma is present in the magnetosphere, and that this plasma exerts a torque on the pulsar, spinning it down faster than in the absence of plasma. If this is indeed the case, then all observable pulsars should have $n < 3$.

Melatos (1997) suggested that the solution to the $n < 3$ problem is related to the angle between the spin and magnetic axes, α , as well as to currents in the magnetosphere. Melatos postulates that the magnetosphere can be considered to be split into two sections, an inner and outer magnetosphere. The division occurs at the ‘vacuum’ radius, the location where particles are no longer confined to field lines. The inner magnetosphere will then corotate with the neutron star and can be considered part of the radius of the rotating dipole. However, since this radius is less than, but comparable in size to, that of the light cylinder, the dipole can no longer be treated as a point, but has some finite size. As a result, $2 < n < 3$ and n approaches 3 as a pulsar ages. This model is especially attractive because it provides an explanation for the large scatter in observed values of n , and provides a prediction for n given measured values of

ν , $\dot{\nu}$ and α . Given the large uncertainties on known values of α , the model roughly agrees with measurements of n for PSRs B1509–58, B0540–69 and the Crab pulsar. PSR J1119–6127 does not appear to have a well determinable α . However, following the Melatos model, the measured value of $n = 2.91 \pm 0.05$ predicts a range of $10^\circ \leq \alpha \leq 32^\circ$ (Crawford & Keim 2003). Our recent measurement of n for PSR J1846–0258 allows a prediction of $\alpha = 8.1 - 9.6^\circ$ (95% confidence). At present, there is no reported radio detection of this source (Kaspi et al. 1996), however, were it one day detected, radio polarimetric observations could in principle constrain α .

8 Conclusions

The five very young pulsars with values of n measured via phase-coherent timing (Table 2) show a wide range of spin properties and behaviors. The glitch behaviour exhibited by these pulsars is widely varied, ranging from PSR B1509–58, which has not glitched in 21.3 yr of continuous timing observations, to the Crab pulsar, which experiences a glitch on average, every ~ 2 yr. The measured values of n for these five pulsars span the relatively wide range between $2.140(9) < n < 2.91(5)$. With the exception of the value of $n = 2.91 \pm 0.05$ for PSR J1119–6127, which is nearly compatible with $n = 3$, the measured values of n are significantly less than 3. The physical cause of the spin-down of pulsars remains one of the outstanding problems in pulsar astronomy.

Acknowledgements This research made use of data obtained from the High Energy Astrophysics Science Archive Research Center Online Service, provided by the NASA-Goddard Space Flight Center. The Molonglo Radio Observatory is operated by the University of Sydney. The Parkes radio telescope is part of the Australia Telescope which is funded by the Commonwealth of Australia for operation as a National Facility managed by CSIRO. MAL is an NSERC PSGS-D Fellow. VMK is a Canada Research Chair. FPG is a NASA Postdoctoral Program (NPP) Fellow. EVG acknowledges NASA ADP grant ADP04-0000-0069. Funding for this work was provided by NSERC, FQRNT, CIAR and CFI. Funding has also been provided by NASA RXTE grants over the course of this study.

References

- Alpar, M.A., Ankay, A., Yazgan, E. ApJL, **557**, L61 (2001)
 Blandford, R., MNRAS **267**, L7, (1994)
 Blandford, R.D. & Romani, R.W. MNRAS **234**, 57, (1988)
 Camilo, F., Kaspi, V.M., Lyne, A.G. et al. ApJ **541**, 367, (2000)
 Contopoulos, I., Spitkovsky, A. **643**, 1139, (2006)
 Crawford, F. & Keim, N.C. ApJ **590**, 1020, (2003)
 Cusumano, G., Massaro, E., & Mineo, T. AAP **402**, 647, (2003)
 Efron, B. The Annals of Statistics **7**, 1, (1979)
 Faucher-Giguère, C.-A. and Kaspi, V. M. ApJ **643**, 332 (2006)
 Gotthelf, E.V., Vasisht, G., Boylan-Kolchin, M., Torii, K. ApJ **542**, L37, (2000)
 Jahoda, K., Swank, J.H., Giles, A.B., et al. Proc. SPIE **2808**, 59, (1996)
 Kaspi, V.M., Manchester, R.N., Siegman, B., et al. ApJ **422**, L83, (1994)
 Kaspi, V. M., Manchester, R. N., Johnston, S., et al. AJ **111**, 2028, (1996)
 Kramer, M., Lyne, A.G., O’Brien, J.T. et al. Science **312**, 549, (2006)
 Livingstone, M.A., Kaspi, V.M., Gavriil, F.P. ApJ **633**, 1095, (2005)
 Livingstone, M.A., Kaspi, V.M., Gavriil, F.P., Manchester, R.N. ApJ **619**, 1046, (2005)
 Livingstone, M.A., Kaspi, V.M., Gotthelf, E.V., Kuiper, L. ApJ, **647**, 1286, (2006)
 Lyne, A.G., Pritchard, R.S., Graham-Smith, F., Camilo, F. Nature **381**, 497, (1996)
 Lyne, A.G., Pritchard, R.S., Smith, F.G. MNRAS **265**, 1003, (1993)
 Manchester, R.N., Durdin, J.M., Newton, L.M. Nature **313**, 374, (1985)
 Manchester, R.N., Mar, D., Lyne, A.G. et al. ApJ **403**, L29, (1993)
 Manchester, R.N., & Taylor, J.H. “Pulsars” Freeman, San Francisco (1977)
 Marshall, F. E. and Gotthelf, E. V. and Middleditch, J. et al. ApJ **603**, 682, (2004)
 McKenna, J. & Lyne, A. G. Nature, **343**, 349 (1990)
 Melatos, A. MNRAS **288**, 1049, (1997)
 Menou, K., Perna, R., Hernquist, L. ApJ **559**, 1032, (2001)
 Michel, F.C., Tucker, W.H. Nature **223**, 277, (1969)
 Ögelman, H. & Hasinger, G. ApJL **353**, L21, (1990)
 Rots, A.: in the proceedings of X-ray Timing 2003: Rossi and Beyond. P. Kaaret, F.K. Lamb, J.H. Swank (eds.) Melville, NY, **714**, 309, (2004)
 Spitkovsky, A. in the proceedings of Astrophysical Sources of High Energy Particles and Radiation. Bulik, T. and Rudak, B. and Madejski, G. (eds.) **801**, 253, (2005)
 Timokhin, A.N. MNRAS **368**, 1055, (2006)
 Zhang, W., Marshall, F. E., Gotthelf, E. V. et al. ApJ **554**, L177, (2001)